CFD modeling of spontaneous heating in a large-scale coal chamber

Liming Yuan[*], Alex C. Smith

Pittsburgh Research Laboratory, National Institute for Occupational Safety and Health, P.O. Box 18070, Cochrans Mill Road, Pittsburgh, PA 15236, USA

A B S T R A C T

Three-dimensional computational fluid dynamics (CFD) modeling is conducted to simulate spontaneous heating in a large-scale coal chamber with a forced ventilation system. Spontaneous heating is modeled as the low-temperature oxidation of coal using kinetic data obtained from previous laboratory-scale spontaneous heating studies. Heat generated from coal oxidation is dissipated by convection and conduction, while oxygen and oxidation products are transported by convection and diffusion. The water vapor transfer and the effect of heat of wetting are not modeled. The CFD model is validated by comparing simulation results with test results from U.S. Bureau of Mines experiments conducted in the coal chamber. The model predicts lower temperatures in the early stage but agrees well on the induction time for spontaneous heating. The effects of airflow rate and order of reaction on the spontaneous heating process are also examined. The calibrated CFD model is found to be useful for predicting the induction time for spontaneous heating in underground coal mines.

1. Introduction

Spontaneous heating of coal occurs when sufficient oxygen is available to sustain the low temperature reaction of coal with oxygen but the heat produced by the coal oxidation is not adequately dissipated by conduction or convection, resulting in a net temperature increase in the coal mass. Coal oxidation is an irreversible exothermic reaction and its reaction rate increases with temperature. The increase in temperature also leads to a higher oxidation rate. If not averted with appropriate action, this process results in thermal runaway and a fire ensues.

Spontaneous heating has long been a problem in the mining, storage, and transport of coal. From 1990 to 1999, approximately 17% of the 87 total reported fires for U.S. underground coal mines were caused by spontaneous heating (DeRosa, 2004). A number of methods have been proposed and used in attempting to predict the spontaneous heating tendencies of coals in laboratory experiments, as reviewed by Carras and Young (1994). Some commonly used methods are crossing point measurements, isothermal and adiabatic calorimetry, oxygen sorption, and temperature differential. In the U.S., the Bureau of Mines developed the minimum spontaneous heating temperature test method using an adiabatic heating oven to predict the relative spontaneous heating tendency to spontaneous heating for U.S. coals (Smith & Lazzara, 1987). Although laboratory results from the above experiments are

valuable, their extrapolation to the large scale, especially the underground mine environment, has not been completely successful because of complicated scaling effects that cannot be reproduced in small-scale experiments. It is both difficult and expensive to conduct large-scale experiments to study spontaneous heating. Most large-scale experiments have attempted to characterize the heat and mass transport properties occurring during spontaneous heating in coal stockpiles. Only two large-scale spontaneous heating tests are available in the literature (Cliff, Clarkson, Davis, & Bennett, 2000; Smith, Miron, & Lazzara, 1991) that are designed to simulate spontaneous heating under actual mine conditions.

Some numerical modeling studies have been done to understand the mechanisms of spontaneous heating (Arisoy & Akgun, 1994; Brooks & Glasser, 1986; Edwards, 1990; Monazam, Shadle, & Shamsi, 1998; Nordon, 1979; Rosema, Guan, & Veld, 2001; Schmal, Duyzer, & van Heuven, 1985; Zarrouk, O'Sullivan, & St. George, 2006). However, these studies are one- or two-dimensional models that mainly focused on small-sized coal stockpiles. Little modeling work has been done simulating actual underground mining conditions. Saghafi and Carras (1997) did numerical modeling of spontaneous heating in an underground coal mine with a ventilation system, but their work was also limited to two dimensions. In this study, a three-dimensional CFD modeling of spontaneous heating of coal, based on the U.S. Bureau of Mines (USBM) large-scale coal chamber tests, was conducted. The coal chamber was built by the USBM to study the spontaneous heating of a large coal mass under conditions that simulate a mined-out area (gob) of a mine (Smith et al., 1991).

[*] Corresponding author. Tel.: +1 412 386 4961; fax: +1 412 386 6595.
E-mail address: lcy6@cdc.gov (L. Yuan).

2. USBM tests

The detailed experimental setup and results from three tests conducted by the USBM in the coal chamber are available in literature (Smith et al., 1991). Here a brief description of the experimental setup is provided to facilitate understanding of the development of the CFD model.

The coalbed chamber is 1.8 m high by 1.8 m wide by 4.5 m long and is preceded and followed by two 1.8-m-high by 1.8-m-wide by 1.2-m-long plenum areas. The schematic of coalbed chamber and plenum areas is shown in Fig. 1.

The sidewalls and floor of the structure are lined with ceramic firebrick. The front and rear walls and the roof of the structure are constructed of 0.16-cm-thick sheet steel. The interior surfaces of the front and rear plenum walls and the plenum roofs are covered with 10 cm of fiberglass blanket insulation. A 1.8-m-high by 1.8-m-wide 0.6-cm-mesh wire screen, reinforced by a 10-cm-mesh wire screen, separates the coalbed from the rear plenum area. The coalbed and front plenum are separated by two 0.9-m-wide by 1.8-m-long, 0.6-cm-mesh wire screens, reinforced by 10-cm-mesh wire screen. The chamber holds up to 12,000 kg of coal and is provided with a forced ventilation system. The ventilation air to the coalbed is provided by two air compressors. The maximum airflow that can be supplied to the coalbed is 200 L/min. Air enters the coal chamber through a 1.3-cm-ID copper tube in the front plenum area, and exits via a 25-cm-ID duct out of the rear plenum.

The temperature histories of the coalbed were recorded using thermocouples arranged in 7 vertical arrays of 9 thermocouples, 0.3, 0.9, 1.5, 2.1, 2.7, 3.4, and 4.0 m from the front of the coalbed, and 3 horizontal arrays of 21 thermocouples, 0.45, 0.9, and 1.35 m above the coalbed floor. Each array contained 9 thermocouples evenly distributed over the surface along the coalbed width direction. Across the width of the coalbed, the thermocouples were located 0.45, 0.9, and 1.35 m from the wall. A gas analysis system was used to monitor the exit gas stream for CH_4, CO, CO_2 and O_2 concentrations, via a 0.9-cm-ID stainless steel gas sampling tube located 0.9 m up into the rear plenum exhaust duct.

Three tests were conducted using different coals and different ventilation conditions during the study. In the first two tests, a sustained heating was not achieved. In the first test, Colorado D seam coal was used with an initial airflow rate of 50 L/min. The airflow rate was reduced to 30 L/min at 9 days, further reduced to 15 L/min at day 58 and lasted to 93 days with a maximum temperature increase of 6 °C. In the second test, Colorado F seam coal was used with an initial airflow rate of 30 L/min. The airflow rate was increased to 50 L/min at 1.8 days, reduced to 25 L/min at 15.7 days, further reduced to 15 L/min at day 57 and lasted to 84.8
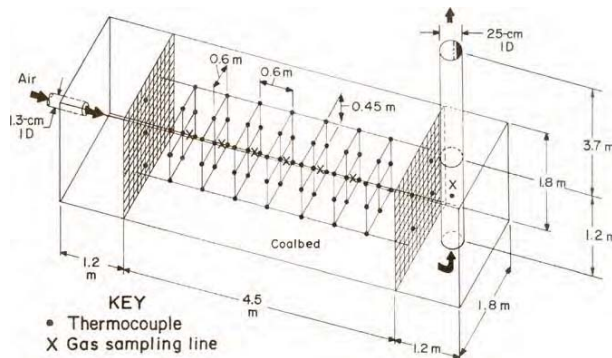

Fig. 1. Schematic of coalbed chamber and plenum areas (Smith, Miron, & Lazzara, 1991).

days with a maximum temperature increase of 9 °C. This paper models the results of the third test with thermal runaway occurring after 23 days. In the third test, hereafter referred to as the USBM test, approximately 12,000 kg of the as-received Wyoming No. 80 coal was crushed to −2 cm. No. 80 coal exhibited a high spontaneous heating potential in laboratory-scale tests (Smith & Lazzara, 1987). 10% of coal was dried and placed from 1.7 to 2.8 m into the coalbed with a height of 0.6–1.5 m above the floor of the coalbed. The rest of the chamber was filled with the as-received coal. The use of dried coal at the center was to expedite the spontaneous heating process. The airflow was 50 L/min at the start, was increased to 100 L/min at 0.8 days, 150 L/min at 7.6 days, and 200 L/min at 21.7 days.

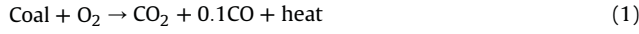## 3. Modeling of low-temperature coal oxidation

The chemical reaction between coal and oxygen at low temperatures is complex. Generally, three types of processes are believed to occur (Carras & Young, 1994): (i) physical adsorption; (ii) chemical adsorption, which leads to the formation of coal-oxygen complexes and oxygenated carbon species; and (iii) oxidation in which the coal and oxygen react with the release of gaseous products, typically carbon monoxide (CO), carbon dioxide (CO_2), and water vapor (H_2O). Of the above processes, oxidation is by far the most exothermic. Physical adsorption can begin at ambient temperature when coal is exposed to oxygen. Chemical adsorption takes place from ambient temperature up to 70 °C. Initial release of oxygenated reaction products starts from 70 to 150 °C, while production of more fully oxygenated reaction produces occurs from 150 to 230 °C. The rapid combustion takes place over 230 °C. The coal temperature rise from ambient temperature to 230 °C is a slow process compared to the rapid temperature increase after 230 °C. In practice, the occurrence of rapid combustion represents a major fire hazard and needs to be prevented if possible. The start of the rapid temperature rise is also called thermal runaway. The time to reach a thermal runaway is called induction time. The induction time can be used to indicate the potential hazard of a spontaneous heating.

The moisture content of coal can play an important role in low-temperature coal oxidation. The interaction between water vapor and coal can be exothermic or endothermic depending on whether the water condenses or evaporates. Sondreal and Ellman (1974) reported that for dried lignite, the rate of temperature rise due to the adsorption of water increased with the moisture content up to a value of 20% water (by mass) and then decreased with further increasing moisture content. Smith and Lazzara (1987) found that, initially, the rate of temperature rise depends on the heat-of-wetting. Later the heating curves pass through an inflection point, in which neither the heat-of-wetting mechanism nor the oxidation mechanism dominates. In the final phase, the oxidation mechanism dominates.

The effect of the moisture content of the air on the spontaneous heating process was also dependent on coal rank and temperature. Smith and Glasser (2005) concluded that adsorption of water vapor does not in itself compete with the low-temperature oxidation in terms of 'heat generation,' but appears to speed up the oxidation rate, and possibly plays a catalytic role. The same conclusion was reached by Smith and Lazzara (1987). In this study, the effect of water vapor is not considered, and only the coal oxidation is simulated.

The chemical reaction between coal and oxygen at low temperature is very complicated and is not well understood. The gaseous reaction products evolved during coal oxidation are primarily CO, CO_2 and H_2O. A little quantity of oxalic acid and mixture of aromatic acids and unsaturated hydrocarbons like C_2H_2,

C_2H_4 and C_2H_6 have also been reported. In this study, it is assumed that CO_2 and CO are the only reaction products from the coal oxidation. The detailed chemical structure of coal varies with the rank and origin of the coal. It is difficult to quantify the exact relationship between the gaseous production rate and the amount of oxygen consumed. According to experimental data (Smith et al., 1991), one mole of coal reacting with one mole of oxygen generates one mole carbon dioxide (CO_2) and roughly 0.1 mole carbon monoxide (CO) plus heat at the early stage of coal oxidation. So the chemical reaction equation can be written as:

$$Coal + O_2 \rightarrow CO_2 + 0.1CO + heat \qquad (1)$$

The dependence of the rate of oxidation, r, on temperature and oxygen concentration can be expressed in the Arrhenius form:

$$r = A[O_2]^n \exp(-E/RT) \qquad (2)$$

where the chemical reaction rate is defined as the rate of change in the concentrations of the reactants and products with a unit of kmol/(m^3 s), A is the pre-exponential factor with a unit of $(kmol/m^3)^{1-n}s^{-1}$, E is the apparent activation energy with a unit of kJ/mol, R is gas constant with a unit of kJ/(mol K), n is the apparent order of reaction, T is the absolute temperature in K, and $[O_2]$ is the oxygen concentration with a unit of kmol/m^3. The value of the apparent order of the reaction, n, in low-temperature oxidation studies of coal and other carbonaceous materials, has been shown to vary from $\sim$0.5 to 1.0 (Carras & Young, 1994), and is about 0.61 for some U.S. coals (Schmidt & Elder, 1940). Using this value, the reaction rate becomes

$$r = [O_2]^{0.61}A \exp(-E/RT) \qquad (3)$$

The value of apparent activation energy, E, of different coals can vary between 12 and 95 kJ/mol. The pre-exponential factor, A, depends more on coal rank and measurement method, and has a typical value between 1 and 7×10^5/s. The values of activation energy and pre-exponential factor for No. 80 coal used in this study were measured by Smith and Lazzara (1987) using an adiabatic heating oven with a temperature range of 20–200 °C. In their study, activation energy and pre-exponential factor were derived using the simple Arrhenius equation

$$\frac{dT}{dt} = A^* \exp(-E/RT) \qquad (4)$$

By plotting the log of the rate of temperature rise, dT/dt, versus $1/T$, the activation energy, E, was determined from the slope as 66.5 kJ/mol and the pre-exponential factor, A^*, from the intercept as 1.9×10^6 K/s. This equation implies a zero order reaction rate. In order to differentiate with the pre-exponential factor A in Eqs. (1) and (3), here A^* was used to denote the pre-exponential factor for the zero order reaction; thus it has a unit of K/s. The relationship between A and A^* can be obtained by an applying the energy balance equation to coal particles

$$\rho_s C_{ps}\frac{dT}{dt} = Q[O_2]^{0.61}A \exp(-E/RT) \qquad (5)$$

where ρ_s is the coal particle density in kg/m^3, C_{ps} is the coal specific heat in J/(kg K) and Q is the heat released during coal oxidation per mole oxygen consumed in kJ/mol-O_2. Substituting Eq. (4) into Eq. (5):

$$\rho_s C_{ps}A^* \exp(-E/RT) = Q[O_2]^{0.61}A \exp(-E/RT)$$

Thus,

$$A = \frac{\rho_s C_{ps}}{Q[O_2]^{0.61}}A^* \qquad (6)$$

The heat generated from oxidation is dissipated by conduction and convection while the oxygen and oxidation products are transported by convection and diffusion. The early stage of spontaneous heating is a slow process, and the gas and coal particles are assumed to be in thermal equilibrium. The detailed modeling of heat transfer is provided in a previous study (Yuan & Smith, 2008).

4. Coal properties and coalbed permeability

The physical and kinetic properties of the coal used in the USBM test and the model are shown in Table 1. The coalbed is treated as a porous medium in the modeling, and the porosity and permeability of the coalbed are used as input in the model. The coalbed is assumed to be evenly packed of coal particles with an average diameter of 2 cm. The porosity of the coalbed was estimated using the equation:

$$\varepsilon = 1 - \frac{\rho_b}{\rho_p}$$

where ρ_b is the coal bulk density and ρ_p is the coal particle density. Using the coal bulk density and particle density of 870 and 1240 kg/m^3, respectively, the estimated porosity is 0.3. Inside the coalbed chamber, the permeability was assumed to be homogeneous and isotropic; the permeability within the coalbed was approximated by the Carmen–Kozeny equation for flow in packed beds (Bird, Stewart, & Lightfoot, 1966):

$$k = \frac{\varepsilon^3 d^2}{150(1-\varepsilon)^2}$$

where d is the particle diameter. Using $\varepsilon = 0.3$ and $d = 0.02$ m, $k = 1.13 \times 10^{-7}$ m^2. The porosity and permeability were assumed to remain constant throughout the coal oxidation reaction.

5. Numerical modeling

A commercial CFD software program, FLUENT[1] from Fluent, Inc., was used in this study to simulate the gas flow and spontaneous heating in the coalbed chamber as well as the gas flow in two plenum areas. FLUENT is a general purpose CFD solver for a broad spectrum of flow, heat transfer and chemical reaction modeling applications. FLUENT can model the mixing and transport of chemical species by solving conservation equations describing convection, diffusion, and reaction sources for each component species. Multiple simultaneous chemical reactions can be modeled, with reactions occurring in the bulk phase and/or on wall or particle surfaces, and in the porous region. In this study, the gas flow in the chamber was treated as laminar flow in a porous medium using Darcy's law. The spontaneous heating of coal was modeled as a surface chemical reaction, coal oxidation, occurring on the coal surface in a porous medium. The heat generated from coal oxidation is dissipated by convection and conduction, while oxygen and oxidation products are transported by convection and diffusion. The generic mass transfer equation solved by FLUENT is reduced to

$$\rho u\frac{\partial Y_i}{\partial x} + \rho v\frac{\partial Y_i}{\partial y} + \rho w\frac{\partial Y_i}{\partial z} = \rho D_i\frac{\partial^2 Y_i}{\partial x^2} + \rho D_i\frac{\partial^2 Y_i}{\partial y^2} + \rho D_i\frac{\partial^2 Y_i}{\partial z^2} + S_i \qquad (7)$$

where Y is the gas component concentration, u, v and w are velocities at x, y, z directions, respectively, μ is gas kinetic viscosity;

Table 1
The physical and kinetic properties of the coal.

Coal particle density	1240	kg/m^3
Coal bulk density	870	kg/m^3
Coal specific heat	1003.2	J/kg-K
Coal conductivity	0.1998	W/m-K
Heat of reaction	300	kJ/mol-O$_2$
Activation energy	66.5	kJ/mol
Pre-exponential factor	1.9×10^6	K/s
Coal particle diameter	2	cm
Initial coal temperature	300	K

k is the permeability of the coalbed, D is the gas diffusion coefficient, S is the rate of species production or consumption and can be calculated based on the rate of reaction. The generic heat transport equation is reduced to

$$\left(\varepsilon\rho_g C_{pg} + (1-\varepsilon)\rho_c C_{pc}\right)\frac{\partial T}{\partial t} + \rho_g C_{pg}\left(u\frac{\partial T}{\partial x} + v\frac{\partial T}{\partial y} + w\frac{\partial T}{\partial z}\right)$$
$$= \lambda_{\text{eff}}\left(\frac{\partial^2 T}{\partial x^2} + \frac{\partial^2 T}{\partial y^2} + \frac{\partial^2 T}{\partial z^2}\right) + rQ \qquad (8)$$

where ε is the porosity, ρ_g, C_{pg} are the density and specific heat for the gas, ρ_c, C_{pc} are the density and specific heat for coal, Q is the heat of reaction of coal oxidation and λ_{eff} is the effective thermal conductivity of the coal matrix. The rate of oxidation, r, is calculated using Eq. (2). The effective thermal conductivity is calculated as:
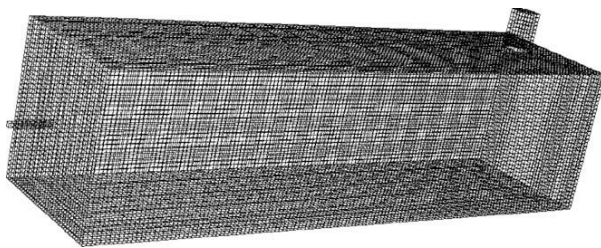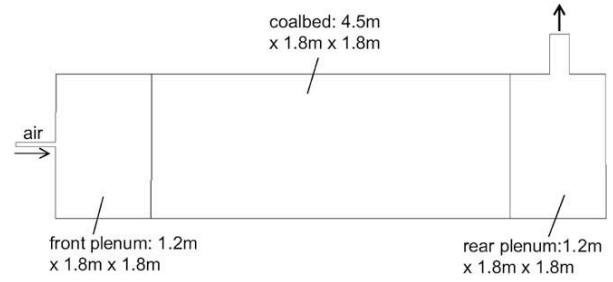
$$\lambda_{\text{eff}} = \varepsilon\lambda_g + (1-\varepsilon)\lambda_c$$

where λ_g and λ_c are the thermal conductivity for gas and coal. Because of the limitation of the FLUENT program, the water vapor transfer and the effect of heat of wetting are not modeled in this study.

The physical model and mesh for the CFD simulation were generated using the mesh generator software, GAMBIT, from Fluent, Inc. Mesh used in the CFD modeling is shown in Fig. 2. The cell size was 5 cm. The total cell number was about 180,000. The geometrical layout for the coalbed chamber and two plenums is shown in Fig. 3.

The input data for the CFD modeling are the initial conditions and boundary conditions. The initial conditions are that the coal and air are all at 300 K. The boundary conditions used in the simulations are the same as the ventilation flows for the USBM test as described in Section 2.

A simulation was conducted first without coal oxidation to obtain steady state flow field and gas distributions in the coalbed chamber and plenum areas. Then, the unsteady simulations with coal oxidation were conducted using the steady state solution as the initial conditions. The initial time step was 1 h, and was reduced to 1 min when significant temperature rise occurred.

Fig. 2. Mesh used in the CFD modeling.

Fig. 3. Geometrical layout for the coalbed chamber and two plenums.
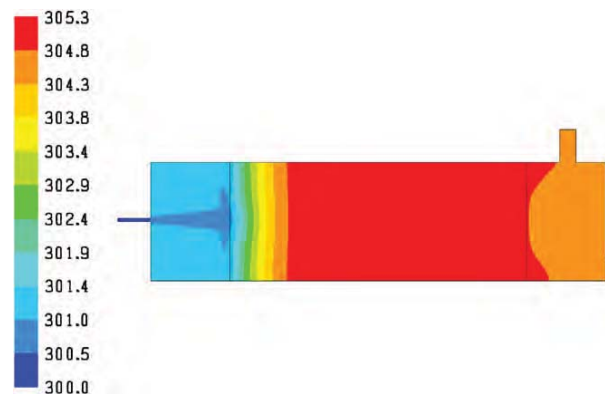
6. Simulation results and discussion

Spontaneous heating can begin at ambient temperature when coal is exposed to oxygen. As the spontaneous heating proceeds, the coal temperature increases slowly. The temperature rise usually consists of two periods. The first period is a slow temperature rise, called the induction period, while the second one is a fast temperature rise. When the coal temperature reaches about 500 K (230 °C), the spontaneous heating mechanism changes to rapid combustion (Babrauskas, 2003). In this study, with the goal of understanding the mechanisms of spontaneous heating, the simulations were focused on the spontaneous heating mechanism at temperatures below 500 K. All simulation results were presented in a vertical center-plane of coalbed chamber and plenums as shown in Fig. 3.

6.1. Simulation results for the development of spontaneous heating process

The simulation results are shown in Figs. 4–10. These results indicate that the development of the heating process in the coalbed can be divided into four stages. During the first stage of spontaneous heating, the temperature rises slowly. Fig. 4 shows the temperature distribution at 8.3 days. The maximum temperature was 305 K, and temperature rise occurred over most of the coalbed. Close to the front plenum, the temperature was slightly lower because of higher air velocity. The oxygen concentration was still at 21% everywhere in the coalbed.

During the second stage, as the temperatures in the coalbed increased, the heat dissipated by the airflow also increased. Because of higher velocity close to the front of the coalbed, more heat was dissipated by the airflow. Thus, the high temperature zone moved back close to the rear plenum. Fig. 5 shows the temperature

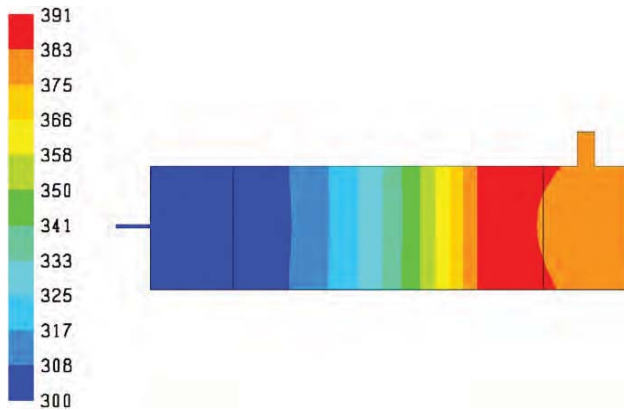**Fig. 4.** Temperature distribution (K) in coalbed chamber and plenum areas at 8.3 days.

Fig. 5. Temperature distribution (K) in coalbed chamber and plenum areas at 24.6 days.

Fig. 7. Temperature distribution (K) in coalbed chamber and plenum areas at 25.6 days.

distribution at 24.6 days. The maximum temperature was 391 K, and the high temperature zone was close to the rear plenum. Fig. 6 shows the oxygen concentration distribution in the coalbed chamber and plenums. Around the high temperature zone, the oxygen concentration was about 2%.

During the third stage, as the rate of temperature rise increased, more oxygen was consumed, leading to insufficient oxygen for coal oxidation close to the rear plenum. Therefore, the high temperature zone started to move toward the front of the coalbed. Fig. 7 shows the temperature distribution at 25.6 days. The maximum temperature was 459 K, and the high temperature was close to the front of the coalbed. Fig. 8 shows the oxygen concentration distribution at 25.6 days. As can be seen, there was nearly no oxygen available downstream away from the high temperature zone.

During the fourth stage, the high temperature zone was limited to a small area close to the center of the front mesh screen as shown in Fig. 9. The maximum temperature was 491 K at 25.8 days. This is because almost all oxygen was consumed in the coalbed as shown in Fig. 10.

6.2. Comparison between simulation results and the USBM test results

Similar phenomena were observed in the USBM test (Smith et al., 1991). In the USBM test, the entire coalbed showed indications of heating immediately after the airflow was started. This temperature increase was probably caused by the heating of
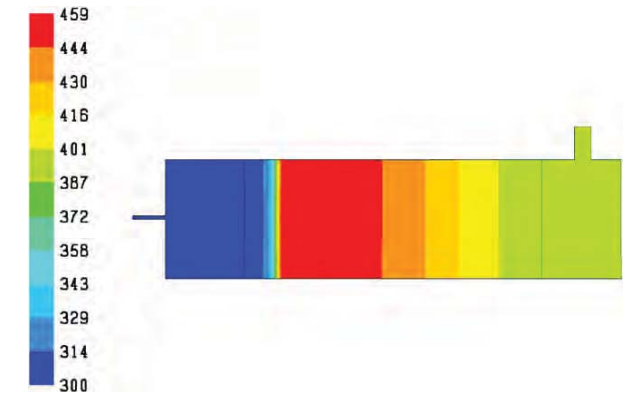
wetting and heat of adsorption. In the USBM test, the thermal runaway occurred near the center of the coalbed after 23 days. The thermal reaction zone then moved toward the front of the coalbed due to oxygen depletion in the center of the coalbed. At 25.3 days, thermal runaway occurred near the front of the coalbed. The simulation results are consistent with these experimental observations.

The simulation results were compared to the USBM test results in Figs. 11–14. In the USBM test, the maximum temperature appeared at the thermocouple 0.3 m from the front of the coalbed and 0.3 m from the floor. Fig. 11 compares the measured temperature at this location with the calculated temperature from the simulation. It can be found that during the induction period, the measured temperature was always higher than that calculated in the simulation. Since about 10% of the total volume of coal was dried before the USBM test, the higher measured temperatures are probably due to the effect of heat of wetting, which is the heat generated by the adsorption of water vapor by the coal surface and is not modeled in the simulation. By comparing the adiabatic oven test results for the same kind of coal, Smith et al. found that the heat of wetting was the dominant mechanism in the early part (first 20 days) in the USBM test. Thermal runaway started roughly at the same time in the USBM test and the simulation. In the simulation, the temperature rose very quickly to about 450 °C, then leveled off for more than one day followed by continual rise again, while in the USBM test, the temperature rose roughly at a constant rate, probably
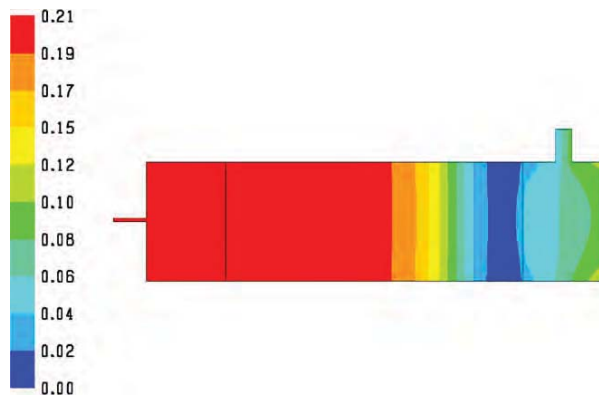

Fig. 6. Oxygen concentration distribution (1 = 100%) in coalbed chamber and plenum areas at 24.6 days.
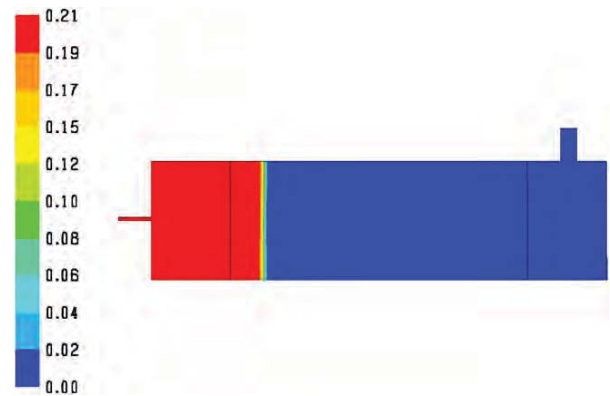

Fig. 8. Oxygen concentration distribution (1 = 100%) in coalbed chamber and plenum areas at 25.6 days.
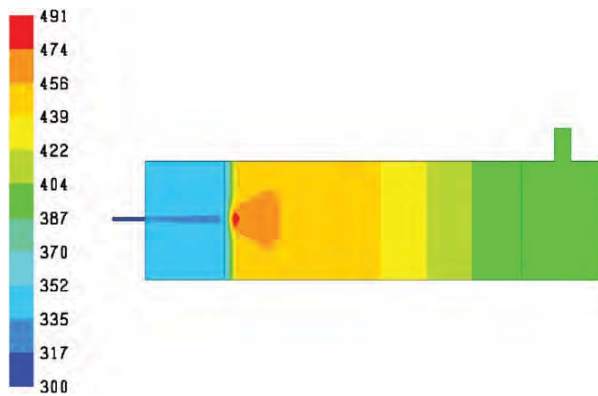
Fig. 9. Temperature distribution (K) in coalbed chamber and plenum areas at 25.8 days.

because of the large logging intervals in the data acquisition system, ranging from 30 min to 4 h.

Fig. 12 compares the temperatures at the location 2.7 m from the front of the coalbed and 0.3 m from the floor. The calculated temperature was also lower than the measured temperature during the induction period at this location. After the start of the thermal runaway, the rate of temperature rise became nearly the same for both measured and calculated temperatures. As discussed by Smith and Lazzara (1987) in their laboratory-scale studies, the heat of wetting is the dominant mechanism at the early stage, but as the temperature rises, the oxidation process becomes the dominant mechanism. Although the adsorption of water vapor was not modeled, the calculated temperatures were in good agreement with the measured values once the coal oxidation process became the dominant mechanism.

The oxygen concentration measured at exit of the 25-cm-ID duct was compared to the calculated value from the simulation, shown in Fig. 13. In the simulation, the oxygen concentration changed minimally during the induction period, while in the USBM test the oxygen concentration decreased to about 17% in the first day. This is because a large amount of oxygen was adsorbed by the coal surfaces at the beginning of the USBM test, and this oxygen adsorption is not modeled in the simulation. As reviewed by Wang, Dlugogorski, and Kennedy (2003), oxygen adsorption includes physical adsorption and chemical adsorption. Physical adsorption is non-specific and somewhat similar to the process of condensation. Chemical adsorption, also called
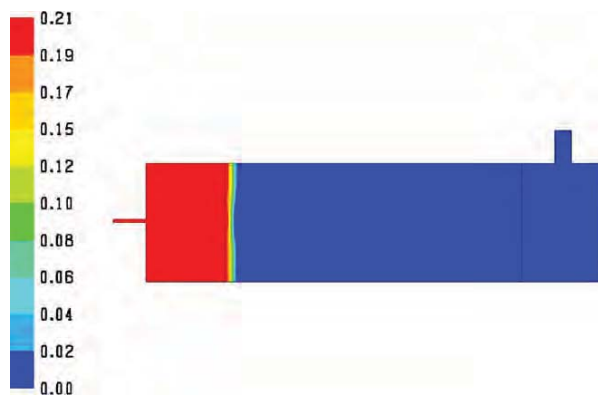

Fig. 10. Oxygen concentration distribution (1 = 100%) in coalbed chamber and plenum areas at 25.8 days.
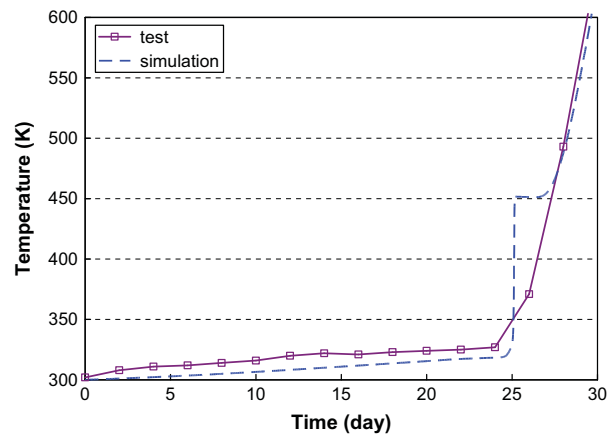

Fig. 11. Comparison between simulation and test for temperature at 0.3 m from the front of the coalbed.

chemisorption, is surface-specific and involves forces much stronger than those operating in physical adsorption. Physical adsorption results in single or multiple layers of adsorbed molecules, while chemisorption is limited to a monolayer of molecules at the pore surfaces.

Initially, oxygen adsorption proceeds at a high rate but after some hours drops off to a slower rate. The oxygen concentration in the simulation decreased quickly to zero after thermal runaway began, characterized by the Arrhenius equation. However, in the USBM test, when the airflow was increased to 200 L/min at 21.7 days, the oxygen concentration first increased from 11% to 12.3%, then slowly decreased to 10%, followed by a quick decrease again. The reason why the increase of airflow to 200 L/min had no effect in the simulation is that oxygen concentration in the simulation was about 20.4% before the airflow rate was increased to 200 L/min, while in the USBM test the oxygen concentration already dropped to about 11% because of oxygen adsorption and coal oxidation.

The CO concentrations from the USBM test and the simulation are compared in Fig. 14. In the USBM test, CO concentration first increased quickly as thermal runaway occurred. When the airflow was increased to 200 L/min, the CO concentration first decreased, probably because of dilution, then increased slightly and leveled off followed by a quick increase again to about 2%. In
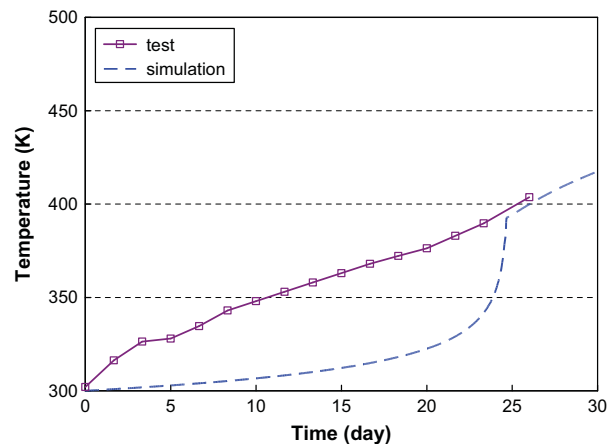

Fig. 12. Comparison between simulation and test for temperature at 2.7 m from the front of the coalbed.
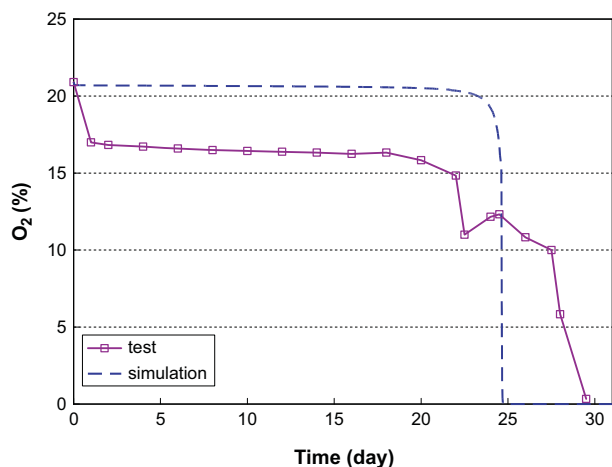
Fig. 13. Comparison between simulation and test for oxygen concentration at exit.

the simulation, once the thermal runaway occurred, the CO concentration increased quickly and leveled at 2.03% eventually, because all the oxygen was consumed by the coal oxidation, and the oxidation rate was completely dominated by the airflow rate.

6.3. Effect of airflow rate

As described in Smith et al. (1991), two additional USBM tests were also conducted in the coalbed chamber before the third one which is simulated in this study. However, a sustained heating was not achieved during the first and second USBM tests. Compared to the third USBM test, the airflow rates were lower in the first and second USBM tests. In the first USBM test, the airflow rate was 50 L/min initially, was changed to 30 L/min at 9 days, and was reduced to 15 L/min at 58 days; in the second USBM test, the airflow rate was 30 L/min initially, was changed to 50 L/min at 1.8 days, was reduced to 25 L/min at 15.7 days, and was reduced to 15 L/min at 57 days. Simulations were conducted to examine the effect of airflow rate on the spontaneous heating. With all parameters kept the same, only the ventilation was changed to the one used in the first and second USBM test, respectively. Fig. 15 shows the temperature histories at 0.3 m from the front of
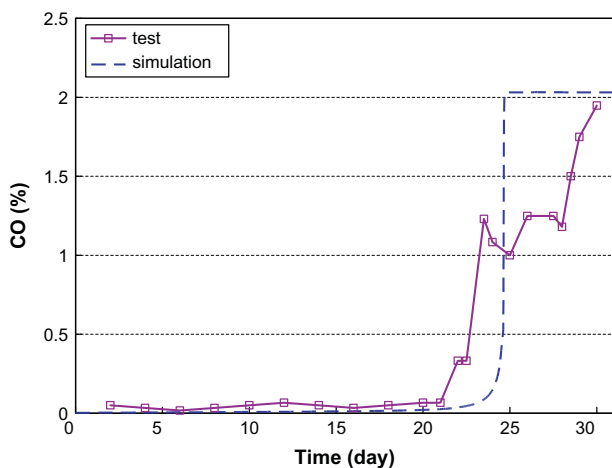
the coalbed for three ventilation conditions. For both ventilation conditions used in the first and second USBM tests, a thermal runaway was reached in the simulations. The induction time was about 50 days for the first USBM test ventilation and about 45 days for the second USBM test ventilation. Although much longer induction times were obtained for the first and second ventilation flows than for the third USBM test ventilation flow, the simulation results indicate that the ventilation was not the reason that thermal runaway was not achieved in the first and second USBM tests. The reason was probably due to the heat-of-wetting of dried coal used in the third USBM test and the increased surface area and weakening of the internal coal structure because of the crushing of the coal just prior to the third experiment.

6.4. Effect of order of reaction

The value of the order of the reaction in low-temperature oxidation studies of coal has been shown to vary from ~0.5 to 1.0 (Carras and Young, 1994). In most mathematical models, the order of reaction is assumed to be equal to 1 in order to simplify the mathematics. In this study, the value used for the order of reaction was 0.61. The order of reaction affects the rate of heat generation, as shown in shown in Eq. (2). Simulations were conducted to examine the effect of the order of reaction on the spontaneous heating. With all parameters kept the same, only the order of reaction was changed to 1 and 0.5, respectively. Fig. 16 shows the temperature histories at 0.3 m from the front of the coalbed for the different orders of reaction. With the order of reaction of 1, after 30 days, the temperature only increased by 2 degrees. With the order of reaction of 0.5, the simulated thermal runaway occurred about 10 days earlier than for the case with the order of reaction of 0.61, indicating that lower order of reaction results in shorter induction time. This is because that once the coal oxidation starts, some oxygen is consumed quickly, leading to lower oxygen concentration locally. With a lower value of order of reaction, the rate of reaction is less dependent on oxygen concentration. Therefore, the rate of reaction increases quickly, leading to an earlier rapid temperature rise, thus a shorter induction time. When the order of the reaction is zero, the rate of reaction is completely independent of the oxygen concentration. With a larger value of order of reaction, the rate of reaction becomes more oxygen concentration controlled. The rate of reaction is reduced because of less oxygen available. Thus, the rate of temperature rise is slowed down, leading to a longer induction time.
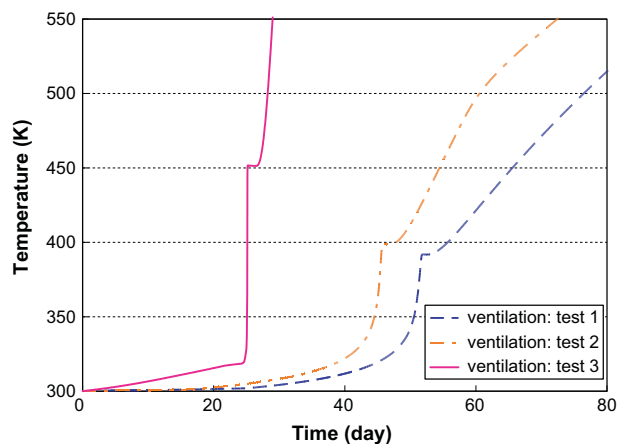

Fig. 14. Comparison between simulation and test for carbon monoxide concentration at exit.

Fig. 15. Temperature histories at 0.3 m from the front of the coalbed for three ventilation conditions.
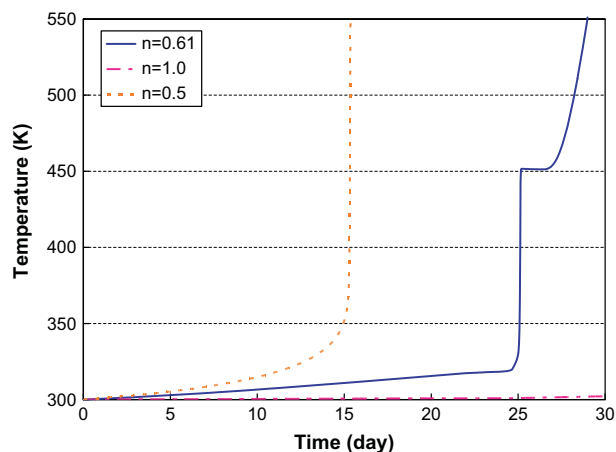
Fig. 16. Temperature histories at 0.3 m from the front of the coalbed for the different orders of reaction.

7. Conclusions

CFD simulations were conducted to model the spontaneous heating of coal in a large-scale coalbed chamber. Simulation results demonstrate that the CFD model reasonably reproduces the major features of spontaneous heating, and the simulation results are in good agreement with the USBM test results. However, the simulated temperatures in coalbed during the induction period were lower than those in the USBM test. This discrepancy is caused by not modeling the effect of water vapor on spontaneous heating. The higher oxygen concentration during the induction period is because of the effect of oxygen adsorption on the coal surfaces, which is also not modeled in the simulations. Although the model predicted lower temperatures and higher oxygen concentrations in the induction stage, the predicted induction time from simulations agrees well with the USBM test results. In real applications, prediction of induction times is very important to prevent spontaneous heating fires, especially in underground coal mines.

Under conditions studied in this work, the higher airflow rate results in a shorter induction time. Simulation results indicate that the airflow rates used in the first and second USBM tests in the coalbed chamber could support thermal runaway with longer induction times if other conditions were the same as in the third USBM test. The order of reaction has a major effect in predicting the induction time. Lower values of order of reaction resulted in the shorter induction times. Under conditions studied here, the value of 0.61 gave a better result compared to values of 0.5 and 1.0.

References

Arisoy, A., & Akgun, F. (1994). Modeling of spontaneous combustion of coal with moisture content included. *Fuel, 73*, 281–286.
Babrauskas, V. (2003). *Ignition handbook*. Issaquash, WA: Fire Science Publishers.
Bird, R. B., Stewart, W. E., & Lightfoot, E. N. (1966). *Transport phenomena*. New York: John Wiley & Sons, Inc.
Brooks, K., & Glasser, D. (1986). A simplified model of spontaneous combustion in coal stockpiles. *Fuel, 65*, 1035–1041.
Carras, J. N., & Young, B. C. (1994). Spontaneous heating of coal and related materials: models, application and test methods. *Progress in Energy and Combustion Science, 20*, 1–15.
Cliff, D., Clarkson, F., Davis, R., & Bennett, T. (2000). The implications of large scale tests for the detection and monitoring of spontaneous combustion in underground coal. 2000 Queensland Mining Industry Health and Safety Conference, 27–30 August 2000, Queensland, Australia.
DeRosa, M. (2004). Analysis of mine fires for all U.S. underground and surface coal mining categories, 1990–1999. *National Institute for Occupational Safety and Health Information Circular, 9470*.
Edwards, J. C. (1990). Mathematical modeling of spontaneous heating of a coalbed. *Report of Investigations 9296*. U.S. Bureau of Mines.
Monazam, E. R., Shadle, L. J., & Shamsi, A. (1998). Spontaneous combustion of char stockpiles. *Energy & Fuel, 12*, 1305–1312.
Nordon, P. A. (1979). A model for the spontaneous heating reaction of coal and char. *Fuel, 58*, 456–464.
Rosema, A., Guan, H., & Veld, H. (2001). Simulation of spontaneous combustion, to study the causes of coal fires in the Rujigou Basin. *Fuel, 80*, 7–16.
Saghafi, A., & Carras, J. N. (1997). Modeling of spontaneous combustion in underground coal mines: application to a gassy longwall panel. In *Proceedings of the 27th International Conference of Safety in Mines Research Institute* (pp. 573–579).
Schmal, D., Duyzer, J. H., & van Heuven, J. W. (1985). A model for the spontaneous heating of coal. *Fuel, 64*, 963–972.
Schmidt, L. D., & Elder, J. L. (1940). Atmospheric oxidation of coal at moderate temperatures. *Industrial and Engineering Chemistry, 32*, 249–256.
Smith, A. C., & Lazzara, C. P. (1987). Spontaneous combustion studies of U.S. coals. *Report of Investigations 9079*. U.S. Bureau of Mines.
Smith, A. C., Miron, Y., & Lazzara, C. P. (1991). Large-scale studies of spontaneous combustion of coal. *Report of Investigations 9346*. U.S. Bureau of Mines.
Smith, M. A., & Glasser, D. (2005). Spontaneous combustion of carbonaceous stockpiles. Part II: factors affecting the rate of the low-temperature oxidation reaction. *Fuel, 84*, 1161–1170.
Sondreal, E. A., & Ellman, R. C. (1974). Laboratory determination of factors affecting storage of North Dakota lignite. *Report of Investigations 7887*. U.S. Bureau of Mines.
Wang, H., Dlugogorski, B. Z., & Kennedy, E. M. (2003). Coal oxidation at low temperatures: oxygen consumption, oxidation products, reaction mechanism and kinetic modeling. *Progress in Energy and Combustion Science, 29*, 487–513.
Yuan, L., & Smith, A. C. (2008). Numerical study on effects of coal properties on spontaneous heating in longwall gob areas. *Fuel, 87*, 3409–3419.
Zarrouk, S. J., O'Sullivan, M. J., & St. George, J. D. (2006). Modeling the spontaneous combustion of coal: the adiabatic testing procedure. *Combustion Theory and Modeling, 10*, 907–926.